ISSN 0003-701X, Applied Solar Energy, 2015, Vol. 51, No. 3, pp. 225–231. © Allerton Press, Inc., 2015.



# Power Efficiency of 5-Blade Drag-Type Vertical Axis Wind Turbine[1]

**M. Zheng, L. Guo, Y. Li, Y. Tian, H. P. Teng, J. Hu, Y. Zhao, and L. J. Yu**

*Institute for Energy Transmission Technology and Application, School of Chemical Engineering, Northwest University, Xi'an, China*

*e-mail: mszheng2@yahoo.com*

Received February 23, 2015

**Abstract**—The computational fluid dynamics (CFD) and computational fluid software FLUENT are employed to simulate the dynamic characteristics of the 5-blade drag-type Vertical Axis Wind Turbine (VAWT), and the power efficiency of drag-type VAWT. In the simulation, the sliding grid and PISO algorithm are used. Different inlet velocity, 6.0, 7.0, 8.0, 9.0, and 10.0 m/s, are employed to investigate the length effect of the simulated region on calculation results of the drag-type VAWT by varying the length of simulation region. It obtained that the critical length of the simulation region and the optimized rotor's rotation rate increase with the inlet wind speed linearly within the scope of this simulation; the relative standard error deceases with the length of simulated range in power function form; the power efficiency of the 5-blade drag-type VAWT increases with inlet wind speed exponentially.

**DOI:** 10.3103/S0003701X15030135

## 1. INTRODUCTION

### *1.1. Status of Research and Application in Wind Turbine*

Modern society accompanies a large amount of energy consumption. Actually, the fossil fuel is limited. The massive exploitation and using of fossil fuel will lead to energy resource exhaustion gradually and it in turn restricts the development of science and technology and social progress [1].

In nowadays, it has been recognized that the increasing exploitation and use of fossil fuels result in serious environmental problems, such as hole in the ozone layer, sea levels rising, and acid rain, etc. In 2005, the Intergovernmental Panel on Climate Change (IPCC) pointed out, the major human emissions of the greenhouse contaminants, including carbon dioxide accounts for roughly 63% of the pollutants, are from carbon dioxide, methane, nitrous oxide and CFCS. In 2008, Energy Information Administration showed that China's emission of carbon dioxide in 2006 accounted to 602 million tons [2], including 495 million tons of carbon dioxide from coal-fired power plant, which equals to 2.05 times that of the global carbon dioxide emissions in 1996, it reaches to the second position in the world [3]. Therefore, the inevitable choice for China is to develop and use the cleanly renewable energy to replace traditional energy sources in the future.

The cleanly renewable energy, including solar energy, wind energy, biomass energy, hydropower, geothermal energy and ocean tidal power, etc, shows a bright potential in the future [4–6]. Among them, wind energy is an inexhaustible renewable energy, widely distributed but low energy density.

The main advantage of wind energy is as follows [7]:

1) Wind energy is always everywhere.

2) Wind energy itself is a kind of very clean and natural energy without pollution.

3) The whole process of wind power generation is pollution free and low energy loss.

There are two kinds of wind turbines generally [8], i.e., horizontal axis wind turbine (HAWT) and vertical axis wind turbines (VAWT), which is divided according to the relative direction of rotor's axis with respect to the inlet wind. Other division methodology is also involved according to the property of the force acting on the blade, i.e., drag-type and lift-type.

HAWT (especially propeller typed) has been used in large wind farms gradually since 1990s, and became the main steam of wind generation. While, VAWT occupies large market share in small wind turbine area. HAWT belongs to the high speed wind turbines, with the high rotation rate in working condition. At the same time, it induces the substantial noise, which affects the daily life of surrounding residents; however, the low speed VAWT induces much smaller noise in their working process. As to this perspective, VAWT is more suitable for ordinary people for direct use of wind power than HAWT.

Savonius's rotor is one of the oldest types of the VAWT. Since the pioneer work of Savonius, it has been studied widely. The advantages of Savonius type are attractive, for example good starting torque, simple mechanism, lower rotation speed, and omnidirectional characteristics [9]. Savonius type wind turbine is

[1] The article is published in the original.

commonly considered as a drag-driven type of wind turbine, which is unlike that of Darrieus type's wind turbines. The general theory of the Savonius turbine is that wind exerts a force on a surface and it results in the surface moving around an axis.

Mahmoud et al. [10] studied the property of Savonius rotor experimentally, it was found that, the effeciency of two-blade rotor is higher than three and four ones, the end plates could raise the efficiency as well. Double stage rotors have higher performance as compared with the single stage rotors. The rotors with overlap are worse than those without overlap in operation. The influence of blade number on power efficiency of Savonius turbine was studied by Zhao et al. [11] numerically, it was found that, the two-blade rotor is more efficient than three ones, and the actual reason for the blade number effect is the "shading effect."

The correlation between the overlap ratio and phase shift angle (installation angle) of double stage three-bladed VAWT was investigated by Kumbernuss et al. [12], it indicated that smaller phase shift angles produce better performance of the turbines at higher air velocities and the larger ones increase the performance at lower air velocities.

In summary, it can be seen that the VAWT has some advantages such as simple structure, low noise, omnidirection, easy starting and installation, etc., it can be used in some special regions [13, 14].

### *1.2. Status of the Computational Fluid Dynamics (CFD) Simulation of Wind Turbine*

**1.2.1. Application status of fluid mechanics calculation method.** The CFD is an efficacious technique to describe the behavior of fluids. In nowadays, it has been frequently used to perform the design and research of machine and production process.

Since 1990s, the progress of CFD has been promoted by the rapid development of computer hardware; the computation technology and its precision are greatly improved as well. Currently, the application of CFD technology has covered almost all fields of human production and living, and a variety of commercial CFD software, such as FLUENT, CFX, Star - cd, Phoenics, etc., has been formed gradually.

**1.2.2. Application of CFD in wind energy area.** With the rapid development of computer technology, the CFD obtains rapid progress; it appears several numerical simulation method, such as, time average method (RANS), large eddy simulation (LES) and direct numerical simulation (DNS). The RANS has mature turbulence model, such as Baldwin-Lomax model, Spalart-Allmara model and $k$–ε model. At the same time, some other general fluid calculation software is also available in the market, such as Fluent, CFX and STAR-CD. In unsteady flow simulation, CFD has been employed to carry out the computation accurately and quickly. The CFD method is more general and intuitive as compared with the stream-tube method and vortex method. By CFD technology using, the flow field around the wind turbine's rotor could be captured accurately; velocity field and pressure field around the rotor could be displayed visually through the visualization technology, so that the aerodynamic performance of rotor could be analyzed accurately.

In the past few years, a numerical simulation of the vortex features around VAWT is conducted by Gregory F. Homicz [15]; 2-D flow field model of the H-type VAWT is analyzed by C.J. Simao Ferreire, et al., they also performed the comparison of the DES (Detaehed-Eddy), LES and RANS calculation models [16]; Nobuyuki Fujisawa et al. performed a numerical simulation of Savonius wind turbine especially the internal flow-field and external flow-field of the blade, and analyzed the influence of the wind speed, tip speed ratio and attack angle on rotor aerodynamic performance [17]. The numerical simulation for Savonius wind turbines is carried out by Burcin Deda Altan and Mehmet Atilgan et al as well, and it pointed out that the CFD technology is applicable in the study of wind turbines pneumatic [18]. In Ref. [19], the effect of simulated region length on simulation results is studied fundamentally, it indicates that the relative standard error of the outline wind speed with respect to that of the infinite position could be less than 5% as long as the simulation scale length is longer than 140 m for a 5-blade VAWT at inlet wind speed 6 m/s, of which the rotor's radius and the blade width are, 2.0 m and 0.76 m, respectively, at the rotation rate 12 rpm. In Ref. [20], the effect of the installation angle of blade on power efficiency of the 5-blade VAWT is studied, it obtained that the maximum power efficiency of 28.48% could be obtained as long as the installation angle is 19° for the turbine with the rotor's radius 2.0 m and the optimized blade width 0.78 m at wind speed of 8 m/s and rotation rate 17 rpm.

Overall analysis of the status of application of the CFD in wind turbine study indicates that the most simulation by the CFD using to analyze windmill features is conducted in the region of 3 to 5 times of the diameter of windmills as the simulation scale up to now, and the discussion concerning the influence of inlet wind speed on the actual efficiency as well as size effect are quite rare [21–24]. However, as is known that the actual efficiency of VATW is important problem concerning the improvement of the turbine design, and the size effect has inevitably significant actions on the calculation result, this kind of study is worth to be done in detail.

In this paper, the CFD is employed to study the variation of power efficiency with respect to wind speed for VATW, and the influence of the simulated region length on the simulation results. In the computation, the general fluid mechanics calculation software FLUENT is combined with the CFD to perform

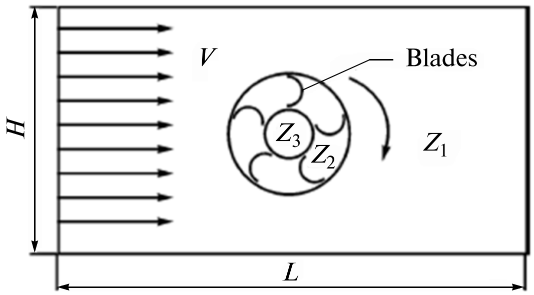


**Fig. 1.** Schematics of calculation region and domain division.

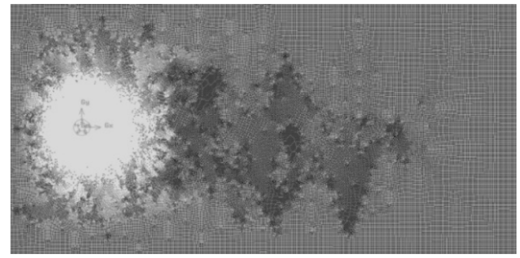

**Fig. 2.** The global Grid.

the numerical simulation for the 5-blade drag-type VAWT.

## 2. FUNDAMENTAL EQUATIONS OF THE FLOW PROPERTY OF WIND FIELD

According to the geometric and operating features of straight blade of VAWT, the flow field of each cross-section along the blade height direction is almost the same, the flow velocity along the blade height direction is approximately zero, therefore the simulation can be simplified into a 2-D flow field so that the amount of calculation could be reduced, and $k$–ε SST turbulence model is employed.

## 3. SIMULATION CALCULATION

For the 5-blade drag-type VAWT, transient calculation is adopt, which differs from SIMPLE algorithm. PISO algorithm is a kind of time division algorithm which was based on the basic variables of pressure [19, 20]. PISO algorithm concerns a multi-step correction in each time step in the transient calculation, so as to ensure the computational efficiency as well as the precision of transient calculation. The turbulence model $k$–ε SST is chosen to perform the simulation, it will ensure to the accuracy of the numerical calculations.

### *3.1. The Geometric Modeling and Mesh Generating of Vertical Axis 5-Blade Drag-Type wind Turbine*

As is mentioned previously, although the real flow field around wind turbine is a 3 dimensional one, the flow field along the blade height is nearly the same excluding at the blade ends, thus 2-dimensional calculation is commonly used to perform the simulation [19, 20]. Figure 1 shows the 2-dimensional computation model. In Fig. 1, three zones are divided for the whole flow field, i.e., $Z_1$, $Z_2$, and $Z_3$. In this division, $Z_3$ is the central circular zone with radius of 1 m, with stationary flow field inside; $Z_2$ is the annular sliding zone with the outer radius of 2.2 m, it includes the 5-blades; $Z_1$ is a rectangular area excluding zones $Z_1$ and $Z_2$. The width and the length of the whole computation region are represented by $H$ and $L$, respectively. Let $V$ and $w$ represent the wind speed and the rotational rate of the turbine, respectively.

The geometric size of wind turbine is as follows, the radius of semicircle blade in the wind turbine is 0.4 m, and the radius of the wind turbine rotor is 2 m. A grid-independence model is employed to carry out the computation for a chosen configuration. The mesh chosen is structure quadrilateral cells; finer at the rotor and rougher at the position far from the rotor, the total number of grid can reach $2.6 \times 10^5$ cells. The sliding zone and the stationary zone are separated by an interface which is two interfaces superposed [15, 16].

In accordance with [19, 20], the calculation region is a rectangular one with the size of $70 \times 140$ m firstly. The wind is inlet with the speed $V$ parallel from the left bound of the calculation region. The turbine center is located 20 m backward from the inlet line of the calculation region.

Each zone has its own borders, while the borders of two concentric circles are overlapped actually. It needs to exchange the calculating data on the overlapped borders during calculations. The number of node around wind blade should be increase adequately. The number of nodes on the each line is shown in Table 1.

The grid "quad" and "pave" are set after node setting is conducted. The global grid and the detailed grid around blade are shown in Figs. 2 and 3, eventually. While, the mesh generation for each zone is shown in Table 2.

### *3.2. Boundary Conditions and Setting of Solvers*

**3.2.1. Boundary conditions.** The "velocity inlet" boundary condition is employed for the inlet one; free flow (outflow) is selected as the outlet boundary con-

**Table 1.** The number of nodes on the each line

| Line | Number of node |
|---|---|
| On each edge of width $H$ | 196 |
| On each edge of length $L$ | 392 |
| Overlapping circle between $Z_1$ and $Z_2$ | 420 |
| Overlapping circle between $Z_2$ and $Z_3$ | 210 |
| Each semicircle blade | 80 |

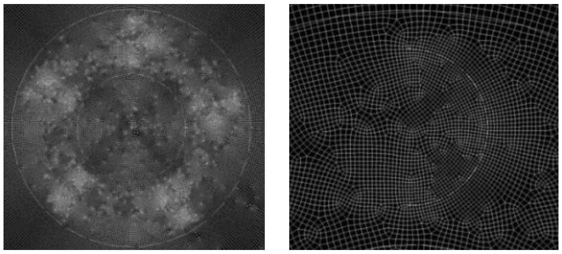


**Fig. 3.** The detailed grid around blade.

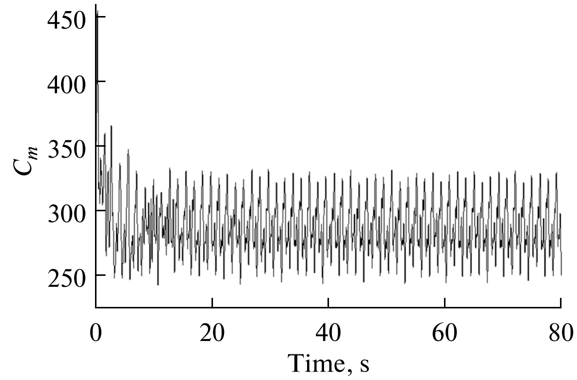


**Fig. 4.** The variation of moment coefficient $C_m$ with respect to time (0–80s).

dition; both sides of the long border is initially symmetrical boundary condition (symmetry); the surface of the blade is set as "wall," blades move together with the sliding zone within $Z_2$, and with the relative speed is 0; interface between zones is set as the "interfacial boundary."

**3.2.2. Setting for solvers.** Transient calculation is employed in the modeling of drag-type 5-blade VATW, it uses pressure—based as the choice of the solving method in FLUENT. For the numerical algorithm of control equations, PISO algorithm is used. The time step is selected as 0.02 s, and calculation is conducted to 4000 steps, therefore the simulation working is 80 s totally every time. The value of moment coefficient ($C_m$) is output at the end of each time step.

**3.2.3. Moment and power efficiency calculation.** Figure 4 desplays the variation of moment coefficient *Cm* with respect to time by using FLUENT software as data processing function. The calculation region is performed in a rectangular region 70 × 140 m. The rotational rate of the rotor is 17 rpm, and wind speed is 8 m/s for a 1 m height 5-blade wind turbine.

The moment coefficient-time curve is the comprehensive result of wind forces applied on the five blades, so the variation of the moment coefficient is oscillated with time frequently. It can be seen from Fig. 4 that the period of moment coefficient is about 7 s. Actually, an averaged value of moment coefficient $C_{mA}$ can be obtained in several periods, and the power of the wind turbine $P$ can be further solved with Eq. (1),

$$P = C_{mA}Cw/60, \quad (1)$$

and the power efficiency is

$$C_v = P/(\rho v^3 hD/2) \quad (2)$$

in which, $C = 0.6125$ is a factor, $w$ represents the rotational rate of the rotor (rad/min), ρ is density of air, $v$ is wind speed, $h$ is the height of the wind turbine, $D$ is diameter of the wind turbine. The term $v^3hD/2$ is the power of the inlet wind.

Under condition of wind speed 8 m/s, rotational speed 17 rpm, and the 1 m height wind turbine, it obtains the averaged torque 176.083 N m from Fig. 4, and thus the power of this drag-type 5-blade VAWT is 313.31 W. While, since the sectional area of the inlet wind is 4 $m^2$, total amount of the wind power in the swept area is $v^3hD/2 = 1254.4$ W, therefore the efficiency of this turbine is 24.98%.

**Table 2.** Mesh generation for each zone

| Zone | Number of grid |
|---|---|
| $Z_1$ | 236562 |
| $Z_2$ | 23316 |
| $Z_3$ | 3877 |
| Total | 263755 |

**Table 3.** Conditions for the simulated computation in case of varying length

| Case no. | 1 | 2 | 3 | 4 |
|---|---|---|---|---|
| The width of the region (m) | 70 | 70 | 70 | 70 |
| The length of the region (m) | 70 | 140 | 210 | 350 |
| The distance from inlet boundary to wind turbine center (m) | 20 | 20 | 20 | 20 |

### *3.3. Length Effect of Simulated Region*

In principle, the calculation region is as bigger as possible. However, big calculation area induces more grid number, and more space and time. Therefore, the size designation for a simulated calculation is a very important, which influences the calculation results significantly.

**3.3.1. Size and grid designation for the 5-blade VAWT.** In [19], it discussed the effect of length of the simulated calculation region on the results, it obtained a conclusion that for a 5-blade VAWT with rotor radius of 2 m and inlet wind speed 6 m/s, the length of the calculating region should be longer than 140 m, so as to keep the relative standard error of wind speeds at the

**Table 4.** The grid number of the 5 varying widths condition

| The size of areas | 70 × 70 m | 70 × 140 m | 70 × 210 m | 70 × 350 m |
|---|---|---|---|---|
| The grid number in $Z_3$ | 3877 | 3877 | 3877 | 3877 |
| The grid number in $Z_2$ | 23771 | 23771 | 23771 | 23771 |
| The grid number in $Z_1$ | 123281 | 246562 | 369843 | 493124 |

exit of region less than 5% as compared with those at the infinite position.

However, there is no report concerning the effect of wind speed on critical length of the calculation region and power efficiency up to now.

In this section, the influence of wind speed on critical length of the calculation region and power efficiency is discussed. The simulation is carried out by varying the length of the calculation region while designating the width of the calculation region as 70 m, the inlet wind speed is selected as 6, 7, 8, 9, and 10 m/s, respectively; the rotational rate changes from 10 to 26 rpm. The designated lengths of the simulation region are listed in Table 3.

In order to make the above 4 cases mutually comparable, the grid number needs to increase with the length correspondingly. As a result, the grid number in $Z_1$ increases at the same partition density, while grid number keeps invariable in zone $Z_2$ and $Z_3$. Finally, it got the grid number for the 5 cases, as shown in Table 4.

**3.3.2. Error analysis.** The usual error analysis method is used to assess the relative error of wind velocity $v_i$ on outline boundary of each point compared to the inlet wind speed $v_0$ for each calculation region. FLUENT software is employed to get the velocity field, as well as the velocity on outline boundary of each point of the every calculation region. Eq. (3) is used to assess the relative error analysis.

$$\delta = \frac{1}{v_0}\sqrt{\frac{\sum_{i=1}^{n}(v_0 - v_i)^2}{n}}, \tag{3}$$

where δ—relative standard errors, $n$—number of data, $v_0$—the wind speed of inlet and infinite locations.

For given inlet wind speed $v_0$, it obtains the wind speed value for each point on the outline boundary $v_i$ for each width of calculation region.

**3.3.2.1. Variation of relative standard error with respect to length of simulation region and inlet wind speed.** Figure 5 presents the variation of relative standard error with respect to length of simulation region at inlet wind speed 7 m/s.

From Fig. 5, it can be seen that the relative standard error decreases in power function form with respect to length of simulated region at inlet wind speed 7 m/s. If 5% is set as the limitation for the relative standard error, 147 m will be the critical length of the simulated region in this case, i.e., in order to keep the relative standard error less than 5%, the length of the simulated region will be longer than 147 m at the wind speed 7 m/s.

Similarly, the critical length of the simulated region at different inlet wind speed could be obtained, it is shown in Fig. 6 under condition of 5% as the limitation for the relative standard error. Figure 6 shows that the critical length of simulated region increases linearly with respect to inlet wind speed. The critical

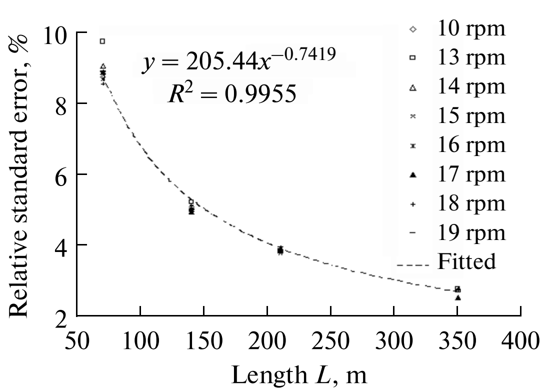


**Fig. 5.** Variation of relative standard error with respect to length of simulated region at inlet wind speed 7 m/s.

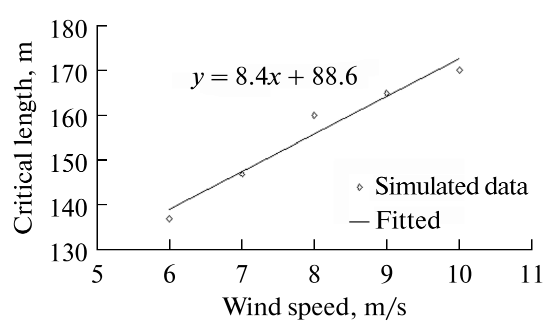


**Fig. 6.** Variation of critical length of simulation region with respect to inlet wind speed.

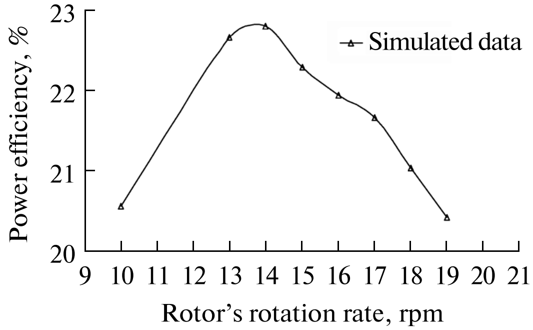


**Fig. 7.** Variation of power efficiency with respect to rotor's rotation rate at inlet wind speed 7 m/s for simulated region of 70 × 210.

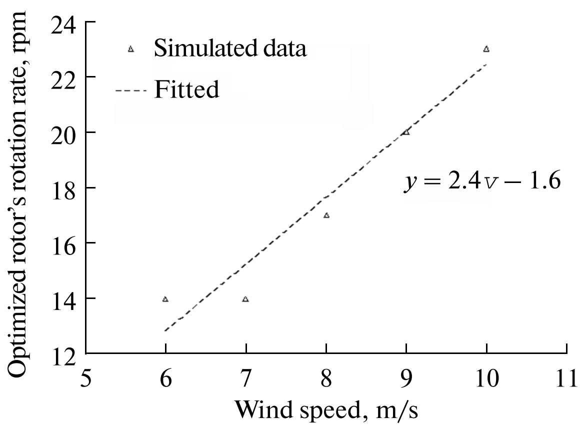


**Fig. 8.** Variation of optimized rotor's rotation rate with respect to inlet wind speed.

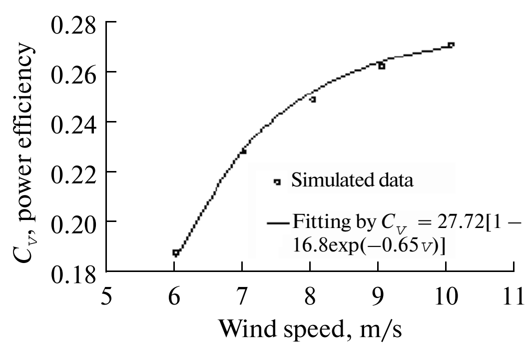


**Fig. 9.** Maximum power efficiency vs different inlet wind speed.

length of simulation region reaches to 170 m for wind speed of 10 m/s.

**3.3.2.2. Variation of power efficiency with respect to inlet wind speed at varying rotation rate of rotor.** In the simulation process, the rotational rate of the rotor could be set for each inlet wind speed, and then the corresponding power efficiency could be obtained. Figure 7 shows the variation of power efficiency with respect to rotor's rotation rate at inlet wind speed 7m/s for simulated region of 70 × 210. The power efficiency is defined as the ratio of the power of rotor received from wind with respect to the power of the inlet wind.

As can be seen that the optimized rotor's rotation rate at inlet wind speed 7 m/s is 14 rpm for simulated region of 70 × 210, at this point the power efficiency reaches to a maximum.

Similarly, the optimized rotor's rotation rate for each inlet wind speed could be obtained for simulated region of 70 × 210, it is shown in Fig. 8, it shows that the optimized rotor's rotation rate increases linearly with respect to inlet wind speed.

Simultaneously, the maximum power efficiency at optimized rotor's rotation rate for each inlet wind speed could be obtained, which is shown in Fig. 9.

As can be seen from Fig. 9 that the maximum power efficiency increases with inlet wind speed exponentially for simulated region of 70 × 210, the variation could be formulated as,

$$C_v = 27.72(1 - 16.18e^{-0.65v}) \tag{4}$$

in which, $C_v$ is the power efficiency, $v$ is inlet wind speed, others are numerically fitted numbers.

From Fig. 9, it can be seen that the maximum power efficiency approaches to its extreme value, 27.72, as wind speed increases to very big value for the simulated region of 70 × 210, it indicates that limitation value of power efficiency for this 5-blade drag type VATW might be 27.72.

## 4. CONCLUDING REMARKS

In conclusion, from above study it found that the critical length of the calculated region increases with the wind speed if the relative standard error of the outline speed 5% is set as the limitation. The critical length of calculated region and the optimized rotor's rotation rate increase linearly with the wind speed in the calculated scopes; the relative standard error deceases with length of simulated range in power function form; the power efficiency of the 5-blade drag-type VAWT increases with inlet wind speed exponentially, the extreme value of power efficiency for this 5-blade drag type VATW might be 27.72.

## ACKNOWLEDGMENTS

This work is supported by the special sci. & tech. innovation program of Shaanxi province and the innovation foundation for postgraduate of Northwest University.

## REFERENCES

1. Fan Yang, Research on the regional difference of energy consumption and its factors, *Doctoral Thesis*, Southwestern University of Finance and Economics, 2008.

2. Gui Xiong, The research on the introduction of carbon tax in China, *Doctoral Thesis,* University of International Business and Economics, 2010.
3. Yuqi Wang, Fusheng Yang, Xiangyu Meng, et al., Simulation study on the reaction process based single stage metal hydride thermal compressor, *Int. J. Hydrogen Energy*, 2010, vol. 35, no. 1, pp. 321–328.
4. Kuanyu Shen, Wind energy resources and wind power generation in China, *J. Northwest Hydropwer,* 2010, vol. 1, pp. 76–81.
5. Qun Zhao, Yongquan Wang, and Hui Li, The current status development trend world wind and power, *Mech. Electr. Eng. Mag.*, 2006, vol. 23, no. 12, pp. 16–18.
6. Baolan Liu and Huali Wen, Current status and prospect of world wind power, *J. Energy Eng.*, 2000, vol. 19, no. 4, pp. 12–14.
7. Jiying Feng, Research on control stratrgies of the megawatt DFIG wind power system, *Doctoral Thesis*, Southwestern Jiaotong Univ., 2010.
8. Chaoqi Jiang and Qiang Yan, Comparative study between horizontal axis and vertical axis wind turbines, *Shanghai Electric Power*, 2007, vol. 2, pp. 163–165.
9. Gupta, R., Biswas, A., and Sharma, K.K., Comparative study of a three-bucket Savonius rotor with a combined three-bucket Savonius-three-bladed Darrieus rotor, *Renew. Energy*, 2008, vol. 33, pp. 1974–1981.
10. Mahmoud, N.H., El-Haroun, A.A., and Wahba, E., An experimental study on improvement of Savonius rotor performance, *Alex. Eng. J.,* 2012, vol. 51, pp. 19–25.
11. Zhao, Z., Zheng, Y., Zhou, D., et al., Optimization of the performance of Savonius wind turbine based on numerical study, *Acta Energ. Solar Sinica*, 2010, vol. 31, pp. 907–911.
12. Kumbernuss, J., Chen, J., Yang, H.X., and Lu, L., Investigation into the relationship of the overlap ratio and shift angle of double stage three bladed vertical axis wind turbine (VAWT), *J. Wind. Eng. Ind. Aerodyn.*, 2012, vol. 107-108, pp. 57–75.
13. Haijiao Tian, Tielong Wang, and Ying Wang, Summarize of the development of the vertical axis wind turbine, *J. Appl. Energy Technol.*, 2006, vol. 11, no. 107, pp. 22–27.
14. Weiyong Chen, VAWT pneumatic design based on CFD numerical simulation, *Doctoral Thesis,* Harbin: Harbin Institute of Technology, 2009.
15. Homicz, G.F., Numerical simulation of VAWT stochastic aerodynamic loads produced by atmospheric turbulence: VAWT-SAL code, *Sandi Report*, 1991, no. SAND91–1124 UC-261.
16. Simao Ferreira, C.S., Bussel, G.J.W., Scarano, F., et al., 2D PIV visualization of dynamic stall on a vertical axis wind turbine, *Proc. 45th AIAA Aerospace Sciences Meeting*, Reno, NV, Jan. 8–11, 2007, pp. 16175–16190.
17. Nobuyuki Fujisawa, Velocity measurements and numerical calculations of flow fields in and around savonius rotors, *J. Wind Eng. Industr. Aerodyn.*, 1996, vol. 59, pp. 39–50.
18. Burcin Deda Altan and Mehmet Atilgan, An experimental and numerical study on the improvement of the performance of savonius wind rotor, *J. Energy Convers. Manag.*, 2008, vol. 49, no. 12, pp. 3425–3432.
19. Yusheng Li, Maosheng Zheng, Haipeng Teng, and Jun Hu, Numerical simulation of 5-blade resistance type vertical axis wind turbines, *Chem. Eng. China.*, 2014, vol. 42, no. 8, pp. 51–55.
20. Maosheng Zheng, Yusheng Li, Yangyang Tian, et al., Effect of blade installation angle on power efficiency of resistance type VAWT by CFD study*, Int. J. Energy Environ. Eng.*, 2014. DOI: 10. 1007/ s40095-014-0142.
21. Yao, Y.X., Tang, Z.P., and Wang, X.W., Design based on a parametric analysis of a drag driven VAWT with a tower cowling, *J. Wind Eng. Ind. Aerodyn.*, 2013, vol. 116, pp. 32–39.
22. Tadjiev, U.A., Kiseleva, E.I., Tadjiev, M.U., and Zakhidov, R.A., Potential of improving energy efficiency of the Andijan HEPP making use of wind farms: part II, *Appl. Solar Energy*, 2013, vol. 49, no. 3, pp. 158–164.
23. Tadjiev, U.A., Kiseleva, E.I., Tadjiev, M.U., and Zakhidov, R.A., Potential of improving energy efficiency of the Andijan HEPP making use of wind farms: part I, *Appl. Solar Energy*, 2013, vol. 49, no. 2, pp. 98–104.
24. Tadjiev, U.A., Kiseleva, E.I., Tadjiev, M.U., and Zakhidov, R.A., Estimated technical and economic indicators of wind power installations that convert wind energy of surface layers of the atmosphere in the plains of Uzbekistan, *Appl. Solar Energy,* 2013, vol. 49, no. 2, pp. 105–109.